

Modelling the expansion of magnetized plasma jets in electric propulsion

M. Merino¹, E. Ahedo¹

¹*Equipo de Propulsión Espacial y Plasmas (EP2), Universidad Carlos III de Madrid, Leganés, Spain*

A semi-analytical fully-magnetized plasma jet model is presented that can be used to rapidly estimate the performances (thrust, efficiency) of 2D and 3D plasma expansions in a magnetic nozzle for space propulsion applications. The model is compared against a complete two-fluid partially-magnetized model, and its range of validity and limitations are assessed and discussed. The 3D plasma expansion in a novel thrust vector control magnetic nozzle is then investigated with the model.

1. Introduction

Magnetized plasma jets are common in several next-generation space electric propulsion technologies, in particular the Helicon Plasma Thruster [1,2] (HPT), the Applied-field MPD [3] (AF-MPD) and the VASIMR [4]. In all these thrusters, a magnetic nozzle (MN) [5] works as the ‘contactless’ acceleration stage. In their usual design, MNs consist of an axisymmetric, convergent-divergent magnetic field that guides the expansion of a hot plasma into a supersonic jet. Inside the MN, the plasma gains axial kinetic energy at the expense of its internal energy, thanks to the self-consistent ambipolar electric field. The reaction to the magnetic forces that shape the plasma expansion are felt on the magnetic circuit of the thruster and generate ‘magnetic thrust’.

In previous work [6,7,8] we have characterized the 2D behaviour of the plasma in a divergent MN. A complete two-fluid model was derived that reproduces the expansion of a plasma with fully magnetized electrons and partially-magnetized or unmagnetized ions. This model requires full numerical integration, and was successfully used to study the acceleration mechanisms, the ambipolar electric field, the development of electric currents in the plasma and the generation of magnetic thrust [6]. The problem of plasma detachment downstream, where the magnetic lines start to turn around and the plasma must continue straight to form a free jet, was discussed in detail in [7], and a clean detachment solution that respects the thrust-generation condition was found in [8]. These results agree with existing laboratory experiments on the suitability of MNs to produce thrust in space propulsion applications.

There is a growing interest in deriving fast, simple models capable of estimating the main plasma properties in the expansion and the propulsive performances of the MN. In this communication, a semi-analytical tool is developed with this purpose, based on the full-magnetization limit of the complete 2D model.

As it turns out, this asymptotic limit renders the model in a very convenient form for integration, and can be readily used in 3D fully-magnetized plasma expansions as well. The model is compared in detail against the general partially-magnetized model, and its range of validity and limitations are discussed in detail. Finally, a novel thrust vectoring magnetic nozzle, termed VECMAN, is analysed using the full-magnetization model.

2. Plasma expansion model

The plasma jet in the MN is assumed to have a clean lateral boundary to vacuum and to be composed of single-charged ions (‘ i ’) and electrons (‘ e ’). The plasma expansion is treated as quasineutral ($n_i \approx n_e \equiv n$), collisionless, and low-beta (i.e., negligible induced magnetic field effects).

Taking the typical orderings in a helicon plasma as a reference, ion temperature is neglected with respect to electron temperature, $T_i \ll T_e$. Electron inertia is neglected with respect to ion inertia. Furthermore, electrons are assumed Maxwellian, isotropic and isothermal. Some of these assumptions can be easily dropped and more complex thermodynamic models for ions and electrons can be adopted [9].

The steady-state expansion are described by the following continuity and momentum equations:

$$\begin{aligned} \nabla \cdot (n\mathbf{u}_i) &= 0; & \nabla \cdot (n\mathbf{u}_e) &= 0; \\ m_i(\mathbf{u}_i \cdot \nabla)\mathbf{u}_i &= -e\nabla\phi + e\mathbf{u}_i \times \mathbf{B} \\ 0 &= T_e\nabla \ln n + e\nabla\phi - e\mathbf{u}_e \times \mathbf{B} \end{aligned}$$

where all symbols are conventional. The model can be normalized with R , the initial plasma jet radius, n_0 , the density at the origin, m_i , e , and T_e .

Without further assumptions, these equations constitute the complete two-fluid model of [6], and the DIMAGNO code can be used to integrate it with the method of characteristics. However, when electrons and ions are assumed to be fully magnetized, the equations can be drastically simplified. This requires, roughly, $\Omega_e, \Omega_i \gg 1$, with Ω_e and Ω_i the dimensionless electron and ion

gyrofrequencies. When these conditions are satisfied, ions and electrons move along magnetic lines with a velocity near the sonic speed, except for a small drift velocity that scales as $O(T_e/eBR)$. According to the scalings above, this drift can be neglected in first approximation, so ion and electron streamlines coincide with magnetic streamlines. The model equations become:

$$\begin{aligned} \mathbf{u}_i &= u_i \mathbf{1}_{\parallel}; & \mathbf{u}_e &= u_e \mathbf{1}_{\parallel} \\ G_i &= nu_i/B; & G_e &= nu_e/B \\ H_i &= \frac{1}{2} m_i u_i^2 + e\phi; & H_e &= T_e \ln n - e\phi \end{aligned}$$

where $\mathbf{1}_{\parallel}$ is the unit vector along \mathbf{B} , and G_i, G_e, H_i, H_e are constants on each magnetic line that can be determined from initial conditions. In summary, we have 4 algebraic equations for 4 unknowns. Given a 2D or 3D external magnetic field, these equations can be readily solved to obtain the full plasma response line by line.

3. Comparison of $\Omega_i \rightarrow \infty$ and $\Omega_i \rightarrow 0$ limits

Clearly, the limit model is only strictly applicable to cases with very high Ω_i . About 400 G are required to magnetize hydrogen ions, and 5000 G to magnetize xenon ions. Hence, it is clear that for the magnetic strength of most practical devices, electrons are well-magnetized while ions are essentially unmagnetized, except perhaps in a small region near the MN throat where the field is stronger. The question naturally arises whether we can use the $\Omega_i \rightarrow \infty$ limit to study practical MN plasma expansions with lower Ω_i , and what is the error committed by this approximation in the calculation of plasma properties and propulsive performance figures.

To study these points, we simulate and compare the $\Omega_i \rightarrow \infty$ and the $\Omega_i \rightarrow 0$ limits for the same

plasma jet. We will call the first simulation the full-magnetization case, and the second the DIMAGNO model under no ion magnetization. Our isothermal plasma is injected sonically in the magnetic field of a single current loop of radius $R_L = 3.5R$. A Gaussian density profile is imposed at the MN throat.

Some of the simulation results are shown in Fig. 1. The differences between the two ion magnetizations are discussed in detail in the presentation. The main points are as follows:

1. Ions detach from the magnetic lines soon after the throat in the $\Omega_i \rightarrow 0$ simulation. This separation is obviously missed in the $\Omega_i \rightarrow \infty$ model, where ion streamlines coincide with magnetic streamlines. Hence, this model is inadequate to study plasma detachment, an important phenomenon in MNs, in partially-magnetized cases. Due to this, an error on ion velocity of about 15% occurs downstream at the periphery.
2. As a consequence of point 1, the radial density profile is more spread out in the $\Omega_i \rightarrow \infty$ simulation. In the full-magnetization limit, n and u_i are only a function of B along each streamline.
3. The ambipolar electric potential ϕ in the fully-magnetized limit is an inaccurate description of the potential in partially-magnetized cases, and using it for these cases can lead to large inconsistencies. The error in $e\phi/T_e$ is given by $\ln n$, so it can be inferred from Fig. 1b. When $\Omega_i \ll 1$, the ion deflection task is performed primarily by the electric force (and in fact, it is insufficient to match the magnetic streamlines, and that is why ion separation occurs). In

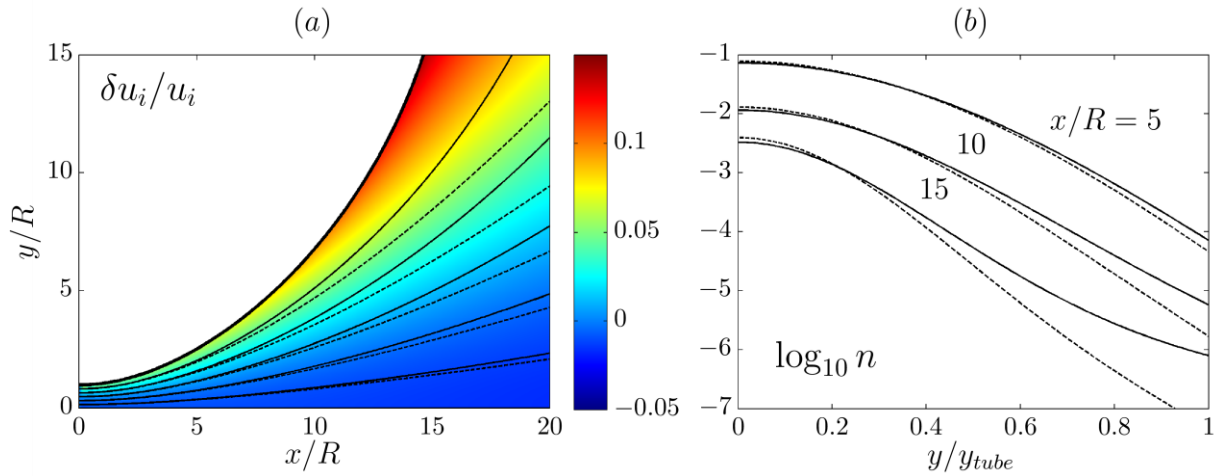


Figure 1. Comparison of the $\Omega_i \rightarrow \infty$ and the $\Omega_i \rightarrow 0$ magnetization limits. (a): Relative difference in ion velocity. Ion streamlines have been drawn. (b): Radial density profile at various axial distances, x . In both graphs, solid lines are for the $\Omega_i \rightarrow \infty$ case and dashed lines for the $\Omega_i \rightarrow 0$ case.

contrast, the deflection in the full-magnetized case is carried out by the magnetic forces alone.

4. For the same reason, ion and electron azimuthal velocities $u_{\theta i}$ and $u_{\theta e}$, are zero in the fully-magnetized model. In fact, we have supplanted the azimuthal and perpendicular momentum equations of the DIMAGNO model with the parallel flow condition. This renders the fully-magnetized model inadequate for the calculation of the key azimuthal plasma currents in a partially-magnetized case. These currents are the essential mechanism for creating and transferring magnetic thrust back to the thruster; nonetheless, magnetic thrust can still be evaluated from a control volume integral of momentum flux.
5. In the fully-magnetized expansion no longitudinal electric currents develop. This is a consequence of the lack of ion separation. If the longitudinal currents are initially, they remain so everywhere. This brings up the local current ambipolarity (LCA) condition, so commonly invoked *a priori* in ambipolar diffusion models. The present comparison shows that in MNs, LCA is only strictly true in the $\Omega_i \rightarrow \infty$ limit.

In spite of these differences, the magnetic thrust force obtained in the MN does not depend much on the value of Ω_i ; this suggests that the fully-magnetized model is a useful simple tool to estimate thrust from a MN in other cases. Nonetheless, the higher the ion magnetization, the lower the thrust gain; therefore, the full-magnetization limit gives a lower bound to the attainable thrust. Care must be put nonetheless when extending this conclusion to 3D cases. A complete 3D model is required to study these effects, and this will be object of future work.

4. 3D plasma jet expansions

Interestingly, new propulsive capabilities can be found when one considers a 3D MN. In this case, a non-axisymmetric convergent-divergent magnetic field guides and expands the plasma jet, but now it also *deflects* it laterally. By controlling the 3D shape of the MN one could, in principle, create a steerable magnetic nozzle (SMN) to orient the plasma jet in any direction within a large angular range.

Figure 2 shows a SMN concept termed VECMAN [10,11]. The VECMAN design can be tailored to produce a deflection of 10, 15 deg or even larger angles, offering added flexibility to any propulsive mission. It can be readily applied to any MN-based thruster, as well as other thrusters without magnetic field or with a nearly-axial magnetic field at the exit like the HEMPT [12] and the DCFT [13].

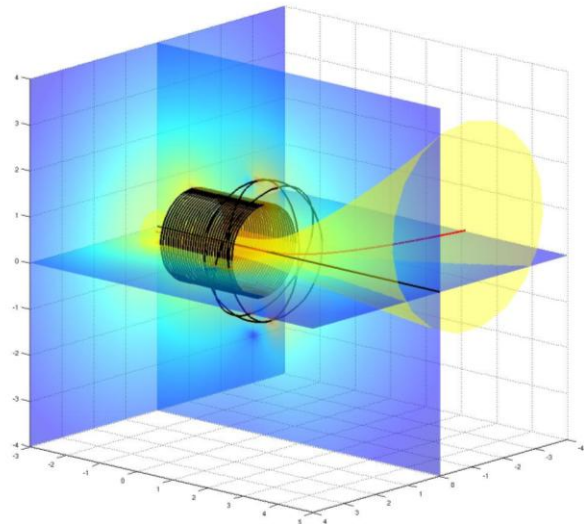


Figure 2. VECMAN steerable magnetic nozzle concept with three tilted magnetic coils, located at the exit plane of a helicon-like plasma source. In yellow, a representative magnetic tube. In red, the magnetic centreline.

This talk will apply the full-magnetized model above to preliminary study the magnetic deflection of the plasma jet in VECMAN.

5. References

- [1] Batishchev, O., "Minihelicon Plasma Thruster," IEEE Trans Plasma Sci, Vol. 37, 2009, pp. 1563-1571.
- [2] Merino, M., Navarro, J., Casado, S., Ahedo, E., Gómez, V., Ruiz, M., Bosch, E., and del Amo, J. G., "Design and development of a 1kW-class helicon antenna thruster," 34th International Electric Propulsion Conference, IEPC-2015-297, 2015.
- [3] Krülle, G., Auweter-Kurtz, M., and Sasoh, A., "Technology and application aspects of applied field magnetoplasma dynamic propulsion," J Propul Power, Vol. 14, 1998, pp. 754-763.
- [4] Diaz, C., "The VASIMR rocket," Sci Am, Vol. 283, No. 5, 2000, pp. 90-97.
- [5] Andersen, S., Jensen, V., Nielsen, P., and D'Angelo, N., "Continuous Supersonic Plasma Wind Tunnel," Phys Fluids, Vol. 12, 1969, pp. 557-560.
- [6] Ahedo, E. and Merino, M., "Two-dimensional supersonic plasma acceleration in a magnetic nozzle," Phys Plasmas, Vol. 17, 2010, pp. 073501.
- [7] Ahedo, E. and Merino, M., "On plasma detachment in propulsive magnetic nozzles," Phys Plasmas, Vol. 18, 2011, pp. 053504.
- [8] Merino, M. and Ahedo, E., "Plasma detachment in a propulsive magnetic nozzle via ion demagnetization," Plasma Sour Sci and Tech, Vol. 23, 2014, pp. 032001.
- [9] Merino, M. and Ahedo, E., "Influence of Electron and Ion Thermodynamics on the Magnetic

Nozzle Plasma Expansion," IEEE Trans Plasma Sci, Vol. 43, No. 1, 2015, pp. 244-251.

[10] Merino, M. and Ahedo, E., "Sistema sin partes móviles ni electrodos y procedimiento para vectorizar el empuje en motores espaciales de plasma," 2013, submitted to the Spanish Patent Office, Patent no. P201331790.

[11] Merino, M. and Ahedo, E., "Towards thrust vector control with a 3D steerable magnetic nozzle," 34th International Electric Propulsion Conference, IEPC-2015-414, 2015.

[12] Kornfeld, G., Koch, N., and Coustou, G., "First Test Results of the HEMP thruster concept," Proceedings of the 28th International Electric Propulsion Conference, 2003.

[13] Courtney, D. and Martínez-Sánchez, M., "Diverging Cusped-Field Hall Thruster," 30th International Electric Propulsion Conference, Florence, Italy, IEPC-2007-39, 2007.